Int. J. Multiphase Flow Vol. 19, No. 4, pp. 541–562, 1993
Printed in Great Britain.

0301-9322/93 $6.00 + 0.00

A MODEL FOR CHOKED FLOW THROUGH CRACKS WITH INLET SUBCOOLING

V. FEBURIE,[1] M. GIOT,[2] S. GRANGER[1] and J. M. SEYNHAEVE[2]

[1]Electricité de France, Département TTA, France

[2]Unité Thermodynamique et Turbomachines, Université Catholique de Louvain, Place du Levant 2, 1348 Louvain-la-Neuve, Belgium

(Received 15 August 1992; in revised form 5 April 1993)

Abstract—The leaks through steam-generator cracks are the subject of research carried out in cooperation between EDF and UCL. A model to predict the mass flow rate has been developed and has been successfully validated. The purpose of the paper is to present this model and to show some comparisons between the results and the presently available data. The model takes into account the persistence of some metastable liquid in the crack and the special flow pattern which appears in such particular geometry. Although the model involves the use of several correlations (friction, heat transfer, ...), no adjustment of parameters against the data has been needed, neither in the single-phase of the flow, nor in the two-phase part.

Key Words: choked flow, cracks, flashing, leak, metastable liquid, speed of sound, steam generator, thermal non-equilibrium, two-phase critical flow

1. INTRODUCTION

In nuclear power plants, some local failures can occur in steam generators. They are due to stress corrosion and they can involve leaks from the primary cooling system to the secondary cooling system. The leak rates are often very low and the cracks are characterized by a relatively short transit time of the fluid, a very short width and a large wall roughness.

The assumption of leak-before-break, i.e. the assumption of the existence of a detectable leakage threshold, is made in relation with the plant operation safety. Continuous operation of the system is allowed until such a threshold is reached. Consequently, it is important to accurately predict the leak rate in a tube wall crack. Such prediction involves the calculation of the critical flow.

At present, there are several ways to determine analytically the critical flow rate through cracks. They are based on Fauske's (1962) model, Moody's (1965) model and Pana's (1976) method. Fauske developed a critical flow model, where the critical flow condition corresponds to a maximum flow rate for the given momentum flux, pressure and quality at the critical section, whereas in Moody's model the maximum flow rate is calculated for the given energy flux, pressure and quality at the critical section. Both models, whose inconsistencies have been demonstrated by Giot & Meunier (1968), assume that the expansion occurs in an equilibrium manner. Pana (1976) proposed a method for calculating the critical mass flow rate with subcooled or saturated water, taking into account the fluid friction in the channel. Thermal equilibrium between the phases is also assumed. The mechanical energy balance equation is used for the liquid phase flow part and the homogeneous equilibrium model, or, alternatively Moody's model describes the two-phase flow part.

John *et al.* (1988) have successfully compared Pana's method with some experimental data obtained with inlet subcooled liquid. However, the use of Pana's method requires the choice between two two-phase models.

Other experimenters, like Nabayashi *et al.* (1991), also use Moody's model under saturated inlet conditions and adjust the crack depth to obtain a good agreement.

Amos & Schrock (1984) described an experimental investigation of the phenomenon in rectangular slits at high pressure and with subcooled stagnation conditions. They proposed a new model including the effects of friction and non-equilibrium flashing. The criterion for flashing inception was based on the Alamgir–Lienhard correlation (Alamgir & Lienhard 1981) and the relaxation of the metastable liquid was assumed to occur exponentially. The agreement between

the model and the data was good for the mass flux prediction; however, the location of the flashing along the flow path, and the pressure drop in the two-phase region were not accurately predicted.

In the present paper, a new simplified model is proposed which calculates the leak rate in a tube wall crack and the pressure distribution along the crack depth for several thermohydraulic conditions. The variation of the cross-section area and the effects of wall friction and wall heat flux are taken into account.

As the water is subcooled in the tubes of a steam generator, i.e. at the crack inlet, bubble nucleation and bubble growth take place inside the crack. Therefore, some degree of thermal non-equilibrium between the liquid and its saturation state can be expected. Several authors have studied the influence of thermal non-equilibrium on the critical flow in pipes or nozzles. Let us mention in particular Lackmé (1979), Bilicki & Kestin (1990), Bilicki *et al.* (1990) and Yan *et al.* (1990, 1991a, b). The applicability of their models in the case of critical flows through cracks needs to be examined. The model proposed in this paper incorporates some of their ideas, especially those expressed in Lackmé's work.

After presenting in section 2 a simplified geometrical model of the cracks, the basic assumptions and balance equations of the flow are written in section 3. The set of equations is complemented by appropriate closure laws. The use of the entropy balance equation appears suitable in the case of the irreversible process of flashing of a metastable liquid: the internal entropy source can be clearly identified, and this helps in understanding the flow evolution. The necessary condition of critical flow is obtained, and the compatibility condition is discussed.

The flow model is the basis of a computer code. The calculation procedure is described and some examples of results are given. A comparison between some available data and the calculated results is presented in section 4. It is concluded that the proposed model enables the prediction of the flow through cracks and offers good potential for interpreting future experimental results.

2. SIMPLIFIED CRACK GEOMETRY

The description of the crack geometry is a basic element necessary to build an analytical model. Cracks cross the tube wall and extend more or less parallel to the tube axis. However, they are very complicated and tortuous. Indeed, the mean surface roughness has the same order of magnitude as the crack width. There are also some local area changes and deviations along the crack depth, but it is difficult to describe them.

Herein the global geometry of the cracks is modeled, whereas the local features are included in the friction factor. As shown in figure 1, the crack is considered as a straight channel, cylindrical, converging or diverging. The crack depth corresponds to the tube wall thickness. The crack width is the smaller dimension (2–500 μm). In practice, it appears that the entrance width is generally smaller than the exit one. In most cases, the crack width is not constant along the crack depth. Therefore, we define a convergent or divergent angle. The large dimension of the crack, that is the crack length, varies between 4 and 15 mm. In this paper, we consider that this length is constant along the crack depth, even if the length at the entrance is in fact slightly larger than at the exit.

The local geometry of the crack which is included in the friction factor takes into account the tortuosity. This global friction factor can be adjusted *a priori* by a single-phase flow experiment.

3. MODEL

3.1. Assumptions

It is assumed that the flow through the cracks involves two parts: a single-phase liquid flow takes place near the crack inlet and extends to a cross section where nucleation starts. The location of the onset of nucleation corresponds to the achievement of some water superheat. Then the steam bubbles grow and eventually coalesce into flat steam pockets (figure 2). The steam pockets are surrounded by saturated liquid, whereas some superheated liquid persists at some distance

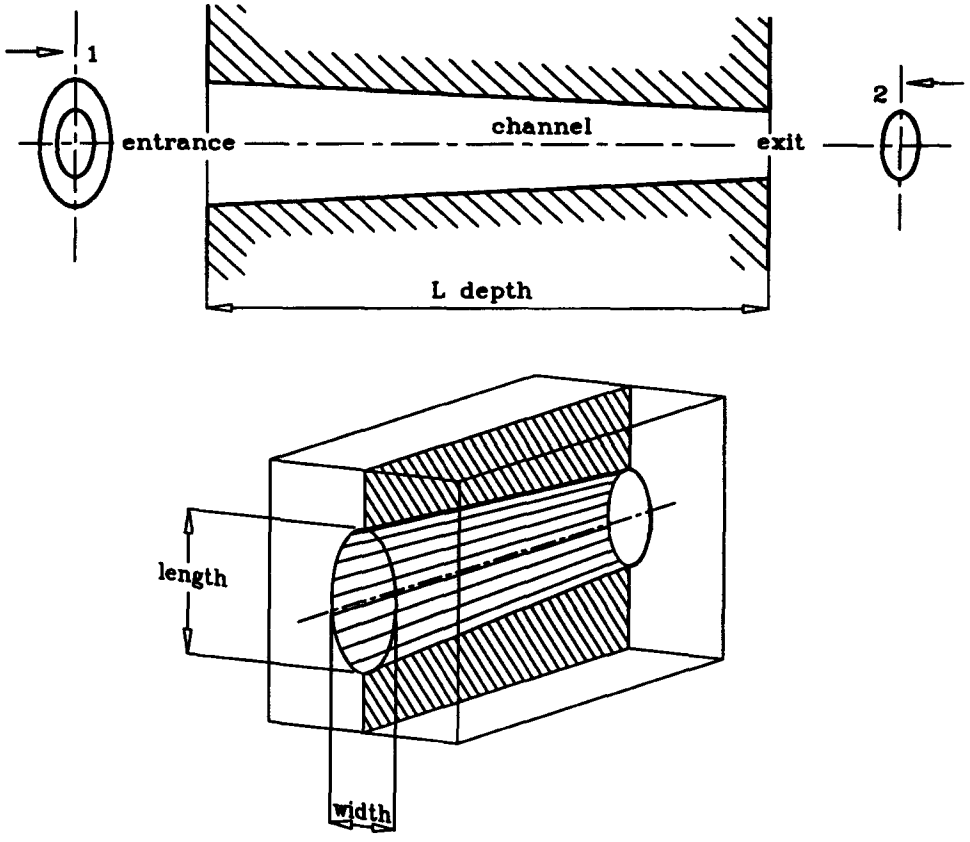

Figure 1. Simplified crack geometry.

between the steam pockets. A typical diagram of the pressure and temperature profiles is shown in figure 3. Typically, the wall temperature T_W decreases by 10°C along the wall thickness (variable z). The liquid enters the crack at a temperature T_L slightly higher than $T_W(0)$, and becomes saturated at a location S where $T_L = T_S(p)$. Beyond this point, the liquid is superheated (metastable). Its temperature T_{LM} goes on decreasing due to wall heat transfer. In the pressure vs thickness diagram, p_e denotes the pressure inside the tube, p is the actual local pressure in the crack and $p_S(T_{LM})$ denotes the saturation pressure corresponding to T_{LM}. The pressure at which the onset of nucleation takes place is denoted p_0, and is somewhat smaller than $p_S(T_{LM})$. Beyond this

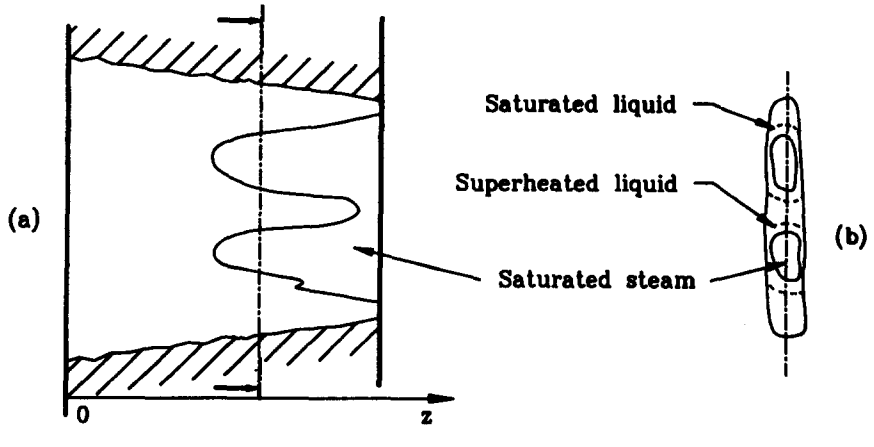

Figure 2. (a) Plane view of a crack; (b) section AA.

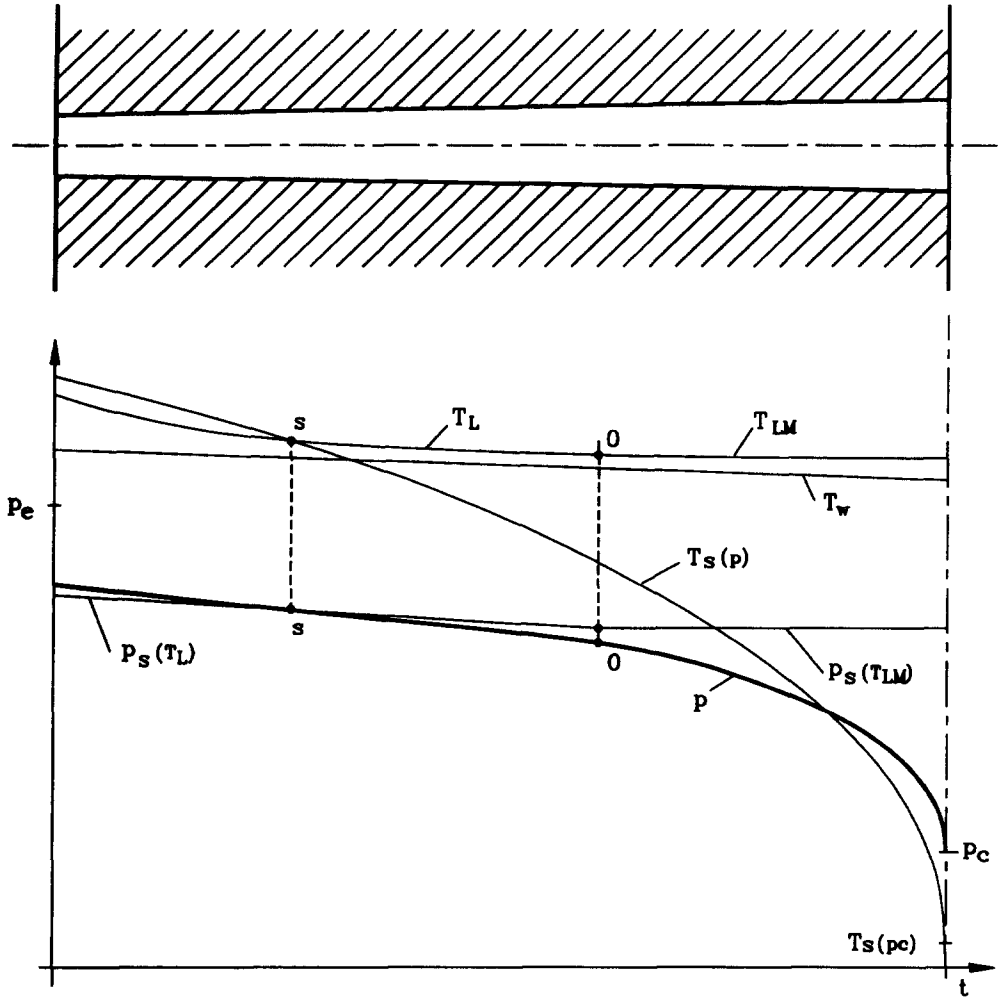

Figure 3. Temperature and pressure profiles along the crack depth.

onset-of-nucleation point, the remaining liquid is supposed to have a more or less constant temperature.

The following set of assumptions A1–A8 enables a simple mathematical model to be developed:

A1. The flow is in steady state.

A2. The fluid consists of three phases: metastable liquid, saturated liquid and saturated steam; the state variables (temperature, pressure) and the velocities being uniformly distributed in each phase at a given cross section.

A3. There is no slip between the phases. This assumption is supported by the piston-like flow.

A4. The liquid is subcooled at the crack inlet. This means that the present model cannot deal with the case where a mixture of liquid and vapour would exist along the inner wall of the tubes. Onset of nucleation is assumed to be reached at pressure p_0, given by the following empirical law (Lackmé 1979):

$$p_0 = k_1 p_S(T_{LM}), \qquad [1]$$

with

$$k_1 = 0.95 \ldots 0.97.$$

A5. For the sake of simplicity, the variation of temperature T_{LM} vs z is neglected beyond the onset of nucleation.
A6. The flow is horizontal.
A7. The resistance to conduction heat transfer in the wall is considered as negligible with respect to the resistance due to convection inside the crack. Hence, the wall temperature is assumed to be independent of the flow in the crack.
A8. Non-uniformities in the direction of the crack length are neglected.

Table 1 presents the consequences of assumptions A1–A3 as well as the definitions of the concentrations of the phases. Note that:

$$\alpha_{LM} + \alpha_{LS} + \alpha_G = 1.$$

3.2. *Single-phase Flow*

Let us consider the single-phase part of the flow, located between the inlet of the crack ($z = 0$) and the onset of flashing ($z = z_0$). The *total pressure drop* is given by the sum of the longitudinal and singular pressure losses:

$$-\Delta p = p(0) - p(z_0) = \Delta p_{long} + \Delta p_{sing}. \quad [2]$$

The longitudinal pressure losses are calculated by the classical expression

$$\Delta p_{long} = \int_0^{z_0} C_f \frac{P_w}{A} \frac{\rho_{LM} w^2}{2} dz,$$

where C_f is the friction factor given by Churchill's correlation (Churchill 1977), P_w is the wetted perimeter, A is the cross-section area and ρ_{LM} is the density of the metastable liquid. The inlet singular pressure losses, including the inlet acceleration term, are given by

$$\Delta p_{sing} = (1 + \xi) \frac{\rho_{LM} w^2(0)}{2},$$

where $\xi = 0.5$ is the head loss coefficient.

The evolution of the temperature of the metastable liquid—and in particular its value at the depth z_0—is given by a simple heat balance:

$$c_p[T_{LM}(z_0) - T_{LM}(0)] = \int_0^{z_0} \frac{h_c P_h [T_w(z) - T_{LM}(z)]}{A \rho_{LM} w} dz. \quad [3]$$

In this equation, h_c denotes the heat transfer coefficient between the flowing liquid and the crack wall, P_h is the heated perimeter ($P_h = P_w$) and c_p is the specific heat of the liquid. The coefficient h_c can be deduced from standard heat transfer correlations like those of Colburn, Sieder and Tate. Then [3] requires a step-by-step integration along the flow path.

The set of equations [2] and [3] is complemented by [1], which enables one to determine z_0 if the mass flow rate ($A \rho_{LM} w$) is known or vice versa (see section 4.1).

3.3. *Balance Equations and Closure Laws for the Region Where $p \leqslant p_0$*

In this region, the flow consists of three phases.

Table 1. Variables and definitions

	Metastable liquid	Saturated liquid	Saturated vapour
Temperature	$T_{LM} = T_{LM}(z)$	$T_{LS} = T_S(z)$	$T_G = T_S(z)$
Pressure	$p_{LM} = p(z)$	$p_{LS} = p(z)$	$p_G = p(z)$
Velocity	$w_{LM} = w(z)$	$w_{LS} = w(z)$	$w_G = w(z)$
Mass fraction	$1 - y$	$(1 - x)y$	xy
Area fraction	α_{LM}	α_{LS}	α_G

3.3.1. Mass balance equations

The mass conservation equations for the metastable liquid (subscript LM), saturated liquid (LS) and saturated vapour (G) are, respectively,

$$\frac{\mathrm{d}}{\mathrm{d}z}(\alpha_{\mathrm{LM}} A \rho_{\mathrm{LM}} w) \equiv -\dot{M}\frac{\mathrm{d}y}{\mathrm{d}z} = \Gamma_{\mathrm{LS/LM}} \qquad [4_{\mathrm{LM}}]$$

$$\frac{\mathrm{d}}{\mathrm{d}z}(\alpha_{\mathrm{LS}} A \rho_{\mathrm{LS}} w) \equiv \dot{M}\frac{\mathrm{d}}{\mathrm{d}z}[(1-x)y] = \Gamma_{\mathrm{LM/LS}} + \Gamma_{\mathrm{G/LS}} \qquad [4_{\mathrm{LS}}]$$

and

$$\frac{\mathrm{d}}{\mathrm{d}z}(\alpha_{\mathrm{G}} A \rho_{\mathrm{G}} w) \equiv \dot{M}\frac{\mathrm{d}}{\mathrm{d}z}(xy) = \Gamma_{\mathrm{LS/G}}, \qquad [4_{\mathrm{G}}]$$

where $\dot{M}$ denotes the mass flow rate and $\Gamma_{i/j}$ is the mass flux per unit length of crack depth from phase i to phase j. By summing up the phasic balance equations, we obtain the three-phase mass balance equation:

$$\sum_k \frac{\mathrm{d}}{\mathrm{d}z}(A\alpha_k \rho_k w) = 0, \quad k = \mathrm{LM, LS, G}. \qquad [4]$$

Introducing the mixture density ρ_{m}, defined by

$$\rho_{\mathrm{m}} \triangleq \sum_k \alpha_k \rho_k,$$

[4] becomes

$$\frac{\mathrm{d}}{\mathrm{d}z}(A\rho_{\mathrm{m}} w) = 0 \qquad [5]$$

or

$$\frac{1}{w}\frac{\mathrm{d}w}{\mathrm{d}z} - \frac{1}{v_{\mathrm{m}}}\frac{\mathrm{d}v_{\mathrm{m}}}{\mathrm{d}z} = -\frac{1}{A}\frac{\mathrm{d}A}{\mathrm{d}z}, \qquad [5']$$

where the volume v_{m} per unit mass, which is a function of x, y, p and T_{LM}, is calculated as

$$v_{\mathrm{m}} \triangleq \frac{1}{\rho_{\mathrm{m}}} = (1-y)v_{\mathrm{LM}} + xyv_{\mathrm{G}} + (1-x)yv_{\mathrm{LS}}. \qquad [6]$$

3.3.2. Momentum balance equations

The momentum balance equations for the metastable liquid, saturated liquid and saturated vapour, are:

$$\alpha_{\mathrm{LM}} A\frac{\mathrm{d}p}{\mathrm{d}z} + \frac{\mathrm{d}}{\mathrm{d}z}(\alpha_{\mathrm{LM}} A \rho_{\mathrm{LM}} w^2) = -P_{\mathrm{W/LM}}\tau_{\mathrm{W/LM}} - \dot{M}w\frac{\mathrm{d}y}{\mathrm{d}z}, \qquad [7_{\mathrm{LM}}]$$

$$\alpha_{\mathrm{LS}} A\frac{\mathrm{d}p}{\mathrm{d}z} + \frac{\mathrm{d}}{\mathrm{d}z}(\alpha_{\mathrm{LS}} A \rho_{\mathrm{LS}} w^2) = -P_{\mathrm{W/LS}}\tau_{\mathrm{W/LS}} + \dot{M}w\frac{\mathrm{d}}{\mathrm{d}z}[(1-x)y] \qquad [7_{\mathrm{LS}}]$$

and

$$\alpha_{\mathrm{G}} A\frac{\mathrm{d}p}{\mathrm{d}z} + \frac{\mathrm{d}}{\mathrm{d}z}(\alpha_{\mathrm{G}} A \rho_{\mathrm{G}} w^2) = -P_{\mathrm{W/G}}\tau_{\mathrm{W/G}} + \dot{M}w\frac{\mathrm{d}}{\mathrm{d}z}(xy), \qquad [7_{\mathrm{G}}]$$

where $P_{\mathrm{W}/k}$ denotes the fraction of the cross-section perimeter occupied by phase k and $\tau_{\mathrm{W}/k}$ is the wall shear-stress of phase k. By summing up the phasic balance equations, we obtain the three-phase momentum balance equation:

$$A\frac{\mathrm{d}p}{\mathrm{d}z} + \sum_k \frac{\mathrm{d}}{\mathrm{d}z}(\alpha_k \rho_k w^2) = -\sum_k P_{\mathrm{W}/k}\tau_{\mathrm{W}/k} \qquad [7]$$

or

$$\frac{dp}{dz} + \frac{1}{A}\frac{d}{dz}(A\rho_m w^2) = -\frac{P_W}{A}\tau_W, \qquad [7']$$

where P_W is the wetted perimeter and τ_W is defined by

$$\tau_W = \frac{\sum_k P_{W/k}\tau_{W/k}}{P_W}.$$

By combining [5] and [7'], one obtains:

$$\frac{dp}{dz} + \rho_m w\frac{dw}{dz} = -\frac{P_W}{A}\tau_W. \qquad [8]$$

3.3.3. Energy balance equations

The energy balance equations for the metastable liquid, saturated liquid and saturated vapour, are

$$\frac{d}{dz}\left[\alpha_{LM}A\rho_{LM}w\left(h_{LM} + \frac{w^2}{2}\right)\right] = P_{h/LM}\dot{q}_{LM} - \dot{M}\left(h_{LM} + \frac{w^2}{2}\right)\frac{dy}{dz}, \qquad [9_{LM}]$$

$$\frac{d}{dz}\left[\alpha_{LS}A\rho_{LS}w\left(h_{LS} + \frac{w^2}{2}\right)\right] = P_{h/LS}\dot{q}_{LS} + \dot{M}\left(h_{LS} + \frac{w^2}{2}\right)\frac{d}{dz}[(1-x)y] \qquad [9_{LS}]$$

and

$$\frac{d}{dz}\left[\alpha_G A\rho_G w\left(h_G + \frac{w^2}{2}\right)\right] = P_{h/G}\dot{q}_G + \dot{M}\left(h_G + \frac{w^2}{2}\right)\frac{d}{dz}(xy), \qquad [9_G]$$

where $P_{h/k}$ denotes the fraction of the heated perimeter occupied by phase k and $\dot{q}_k$ the wall heat flux to phase k. By summing up the phasic balance equations, we obtain the three-phase energy balance equation:

$$\sum_k \frac{d}{dz}\left[\alpha_k A\rho_k w\left(h_k + \frac{w^2}{2}\right)\right] = P_h\dot{q}_w, \qquad [9]$$

where P_h is the heated perimeter and $\dot{q}_W$ is defined by

$$\dot{q}_W = \frac{\sum_k P_{h/k}\dot{q}_k}{P_h}.$$

Let us define the mixture enthalpy per unit mass as

$$h_m \triangleq \frac{1}{\rho_m}\sum_k \alpha_k\rho_k h_k.$$

Then, using [5], [9] can be rewritten in the form

$$\frac{d}{dz}\left(h_m + \frac{w^2}{2}\right) = \frac{\dot{q}}{\dot{M}}. \qquad [10]$$

We note that the mixture massic enthalpy, which is a function of x, y, p and T_{LM}, can be calculated by the following expression:

$$h_m = (1-y)h_{LM} + xyh_G + (1-x)yh_{LS}. \qquad [11]$$

3.3.4. Entropy balance equations

The entropy balance equation for the metastable liquid is

$$\frac{d}{dz}(\alpha_{LM}A\rho_{LM}ws_{LM}) = -\dot{M}s_{LM}\frac{dy}{dz} + \dot{M}(1-y)\frac{ds_{LM}}{dz}, \qquad [12_{LM}]$$

with

$$T_{LM}\frac{ds_{LM}}{dz}=\frac{dh_{LM}}{dz}-\frac{1}{\rho_{LM}}\frac{dp}{dz}. \qquad [13_{LM}]$$

From $[9_{LM}]$ combined with $[4_{LM}]$, one may derive

$$\frac{dh_{LM}}{dz}=\frac{P_{h/LM}\dot{q}_{LM}}{(1-y)\dot{M}}-w\frac{dw}{dz}; \qquad [14_{LM}]$$

and $[7_{LM}]$ combined with $[4_{LM}]$ leads to

$$\frac{dp}{dz}=-\frac{P_{W/LM}\tau_{W/LM}}{\alpha_{LM}A}-\rho_{LM}w\frac{dw}{dz}. \qquad [15_{LM}]$$

Hence, $[13_{LM}]$ can be written as

$$T_{LM}\frac{ds_{LM}}{dz}=\frac{P_{h/LM}\dot{q}_{LM}}{(1-y)\dot{M}}+\frac{P_{W/LM}\tau_{W/LM}}{\alpha_{LM}A\rho_{LM}} \qquad [16_{LM}]$$

and, finally, $[12_{LM}]$ becomes

$$\frac{d}{dz}(\alpha_{LM}A\rho_{LM}ws_{LM})=-\dot{M}s_{LM}\frac{dy}{dz}+\frac{P_{h/LM}\dot{q}_{LM}}{T_{LM}}+\frac{w}{T_{LM}}P_{W/LM}\tau_{W/LM}. \qquad [17_{LM}]$$

Following a similar procedure for the saturated liquid, one obtains

$$\frac{d}{dz}(\alpha_{LS}A\rho_{LS}ws_{LS})=\dot{M}s_{LS}\frac{d}{dz}[(1-x)y]+\frac{P_{h/LS}\dot{q}_{LS}}{T_S}+\frac{w}{T_S}P_{W/LS}\tau_{W/LS}; \qquad [17_{LS}]$$

and for the saturated vapour, one can write

$$\frac{d}{dz}(\alpha_{G}A\rho_{G}ws_{G})=\dot{M}s_{G}\frac{d}{dz}(xy)+\frac{P_{h/G}\dot{q}_{G}}{T_S}+\frac{w}{T_S}P_{W/G}\tau_{W/G}. \qquad [17_{G}]$$

By summing up the phasic entropy balance equations, one obtains the three-phase entropy balance equation:

$$\frac{d}{dz}\sum_k(\alpha_kA\rho_kws_k)=\dot{M}(s_{LS}-s_{LM})\frac{dy}{dz}+\dot{M}(s_G-s_{LS})\frac{d}{dz}(xy)+\sum_k\frac{P_{h/k}\dot{q}_k}{T_k}+w\sum_k\frac{P_{W/k}\tau_{W/k}}{T_k}. \qquad [17]$$

As the heat corresponding to the transfer of a mass flux $\dot{M}\,dy$ from the metastable phase to the saturated liquid is equal to the vaporization heat, we can write

$$\dot{M}h_{lv}\frac{d}{dz}(xy)=\dot{M}(h_{LM}-h_{LS})\frac{dy}{dz}, \qquad [18]$$

and hence, [17] becomes

$$\frac{d}{dz}\sum_k(\alpha_kA\rho_kws_k)=\dot{M}(s_{LS}-s_{LM})\frac{dy}{dz}+\dot{M}\frac{h_{LM}-h_{LS}}{T_S}\frac{dy}{dz}+\sum_k\frac{P_{h/k}\dot{q}_k}{T_k}+w\sum_k\frac{P_{W/k}\tau_{W/k}}{T_k}. \qquad [19]$$

The first two terms on the r.h.s. of [19] consist in an "internal" entropy source $\Delta_{IS}\,(dy/dz)$ due to the irreversible process involving the mass transfer from the metastable to the saturated liquid phase on the one hand,

$$\dot{M}(s_{LS}-s_{LM})\frac{dy}{dz}=\dot{M}c_{pL}Ln\frac{T_S}{T_{LM}}\frac{dy}{dz},$$

and the heat transfer associated with this mass transfer through a temperature discontinuity on the other hand,

$$\dot{M}\frac{h_{LM}-h_{LS}}{T_S}\frac{dy}{dz}=\dot{M}c_{pL}T_{LM}\left(\frac{1}{T_S}-\frac{1}{T_{LM}}\right)\frac{dy}{dz}.$$

The sum $\Delta_{IS}\,(dy/dz)$ is always positive or zero.

The last two terms on the r.h.s. of [19] consist of an "external" entropy flux due to wall heat flux and an "external" entropy source due to wall friction. The sum is denoted Δ_{ES}. Let us define the mixture entropy per unit mass by

$$s_m \triangleq \frac{1}{\rho_m} \sum_k \alpha_k \rho_k s_k .$$

Then [19] can be written as

$$\frac{d}{dz}(A\rho_m w s_m) = \Delta_{IS}\frac{dy}{dz} + \Delta_{ES} \qquad [20]$$

or, using [5], one obtains

$$\frac{ds_m}{dz} = \frac{1}{\dot{M}}\left(\Delta_{IS}\frac{dy}{dz} + \Delta_{ES}\right). \qquad [20']$$

The mixture massic entropy, which is a function of x, y, p and T_{LM}, can be calculated as

$$s_m = (1-y)s_{LM} + xys_G + (1-x)ys_{LS}. \qquad [21]$$

3.3.5. A practical set of equations

If we assume that $\tau_{W/k}$ and $\dot{q}_k$ depend only on the variables, and not on their gradients, the set of equations [5'], [7'] and [20'], complemented by an equation of state

$$v_m = v_m(p, s_m, y), \qquad [22]$$

and by a closure law for y

$$\frac{dy}{dz} = f(p, y, T_{LM}), \qquad [23]$$

can be written in a matrix form:

$$\begin{bmatrix} 0 & 1 & -\frac{w}{v_m} & 0 & 0 \\ 1 & \frac{w}{v_m} & 0 & 0 & 0 \\ \frac{\partial v_m}{\partial p} & 0 & -1 & \frac{\partial v_m}{\partial s_m} & \frac{\partial v_m}{\partial y} \\ 0 & 0 & 0 & 1 & -\frac{\Delta_{IS}}{\dot{M}} \\ 0 & 0 & 0 & 0 & 1 \end{bmatrix} \begin{bmatrix} \frac{dp}{dz} \\ \frac{dw}{dz} \\ \frac{dv_m}{dz} \\ \frac{ds_m}{dz} \\ \frac{dy}{dz} \end{bmatrix} = \begin{bmatrix} -\frac{w}{A}\frac{dA}{dz} \\ -\frac{P_W}{A}\tau_W \\ 0 \\ \frac{\Delta_{ES}}{\dot{M}} \\ f(p, y, T_{LM}) \end{bmatrix}. \qquad [24]$$

3.3.6. Closure laws

3.3.6.1. Saturated steam–water mixture fraction. In addition to τ_w and $\dot{q}_w$, which have to be determined by some two-phase flow friction and heat transfer correlations (see below), a closure law is used to define the evolution of the saturated steam–water mixture fraction y along the crack (Hardy & Mali 1983):

$$\frac{dy}{dz} = k(1-y)\left[\frac{p_S(T_{LM}) - p}{p_{crit} - p_S(T_{LM})}\right]^{1/4}, \qquad [25]$$

where p_{crit} is the pressure at the critical point and k is a constant for a given pipe geometry. According to this expression, the fraction dy of liquid which is transferred from the metastable phase to the saturated liquid phase per unit length is proportional to the remaining quantity of metastable liquid $(1-y)$ and to some function of the metastability expressed by means of a pressure difference.

As the nucleation sites lie mainly in wall microcavities, it is assumed that different pipe geometries and wall roughnesses would lead to different values of the constant k. For example, assuming the same material, the number of active sites per unit volume V of pipe is proportional to the wall surface S_W. Therefore, we suppose that k is proportional to the ratio

$$\frac{S_W}{V} = \frac{\int P_W \, dz}{\int A \, dz}.$$

Using the data resulting from the Moby-Dick experiments, one obtains $k = 4$ for a cylindrical pipe having a ratio $P_W/A = 200\,m^{-1}$. For other geometries, we propose to use

$$k = k_2 \frac{P_W}{A} \quad \text{with } k_2 = 0.02.$$

Due to the lack of experimental evidence, the dependence of k_2 with respect to the roughness is not taken into account explicitly in this expression.

Equation [25] can be compared to the relaxation equation proposed by Bilicki & Kestin (1990). Let us define the quality:

$$X \triangleq xy.$$

Then, [18] can be integrated at a given pressure between an equilibrium state characterized by a value $\bar{X}$ of the quality and $y = 1$ on the one hand and the actual non-equilibrium state on the other hand:

$$h_{lv}(X - \bar{X}) = -(h_{LM} - h_{LS})(1 - y).$$

This equation can be written as

$$X - \bar{X} = -\Delta h^*(1 - y),$$

where Δh^* denotes a non-dimensional quantity similar to the Jakob number

$$\Delta h^* = \frac{h_{LM} - h_{LS}}{h_{lv}}.$$

Equation [25] becomes

$$\frac{dy}{dz} = \frac{d}{dz}[\Delta h^{*-1}(X - \bar{X})] = -k(X - \bar{X})\Delta h^{*-1}\left(\frac{p_S - p}{p_{crit} - p_S}\right)^{1/4}. \qquad [26]$$

If we accept the two following approximations:

$$\Delta h^* = \text{const} \quad \text{and} \quad \bar{X} = \text{const},$$

which clearly correspond to the flashing of a stagnant fluid otherwise Δh^* and X would depend on the local value of the pressure, which would depend on the coordinate, then [26] yields

$$\frac{dX}{dz} = -k\left(\frac{p_S - p}{p_{crit} - p_S}\right)^{1/4}(X - \bar{X}).$$

This expression can be identified to the relaxation equation whose use has been proposed by Bilicki & Kestin (1990),

$$\frac{dX}{dz} = \frac{X - \bar{X}}{w\theta},$$

by writing

$$k\left(\frac{p_S - p}{p_{crit} - p_S}\right)^{1/4} = \frac{1}{w\theta}.$$

By introducing $w = dz/dt$, we obtain

$$\frac{dX}{dt} = \frac{X - \bar{X}}{\theta}.$$

The above development suggests that the validity of Bilicki & Kestin's relaxation equation could be limited to the flashing of a liquid moving in isobaric conditions. The structure of [26] is better suited for a flowing fluid subject to flashing.

3.3.6.2. Wall shear stress. Three correlations for predicting the gas–liquid friction pressure gradient have been used and compared in the present study:

(i) The *Lockhart–Martinelli correlation*, modified by Richardson, which yields

$$\Phi_L^2 = (1 - \alpha_G)^{-1.75}, \quad [27]$$

where Φ_L^2 denotes the ratio between the gas–liquid friction pressure gradient and the single-phase friction pressure gradient where the liquid flows at the same flow rate as in the multiphase flow.

(ii) *Chisholm's correlation*

$$\Phi_{LO}^2 = 1 + (\tau^2 - 1)\{B[X(1 - X)]^{(2-n)/2} + X^{2-n}\}, \quad [28]$$

where Φ_{LO}^2 denotes the ratio between the gas–liquid friction pressure gradient and the single-phase friction pressure gradient when the liquid flows at velocity w. The other parameters are defined as follows:

$$B \triangleq \frac{21\tau - 2^{2-n} + 2}{\tau^2 - 1},$$

$$\tau^2 \triangleq \left(\frac{\rho_L}{\rho_G}\right)\left(\frac{\mu_G}{\mu_L}\right)^n$$

and

$$n = 0.25.$$

(iii) A correlation proposed for *capillary tubes* by Lin *et al.* (1989) and based on Churchill's correlation for single-phase flow, the Reynolds number being calculated with a mixture viscosity μ_m:

$$\mu_m \triangleq \left[\frac{1}{\mu_L} + X^{1.4}\left(\frac{1}{\mu_G} - \frac{1}{\mu_L}\right)\right]^{-1}. \quad [29]$$

3.3.6.3. Wall heat transfer. Three correlations have been tested for the prediction of the wall heat flux:

(a) *Chen's (1966) correlation.* The two-phase gas–liquid heat transfer coefficient h_{TP} is given by

$$h_{TP} = h_c F + h_b S, \quad [30]$$

where h_c and h_b refer, respectively, to convection and nucleate boiling, and F and S are weighting factors. The convection coefficient is calculated by the Dittus–Boelter correlation, whereas the nucleate boiling coefficient is determined from Forster–Zuber's correlation. The factor F is expressed as a function of the Martinelli parameter X_{tt}:

$$F = \begin{cases} 1 & \text{if } X_{tt}^{-1} < 0.1 \\ 2.35(X_{tt}^{-1} + 0.213)^{0.736} & \text{if } X_{tt}^{-1} \geqslant 0.1. \end{cases}$$

Finally,

$$S = (1 + 2.53 \times 10^{-6}\, \mathrm{Re}_{TP}^{1.17})^{-1},$$

with

$$\mathrm{Re}_{TP} \triangleq F^{1.25}\, \mathrm{Re}_L.$$

(b) *Klimenko's (1988) correlation.* This correlation is as follows:

$$\mathrm{Nu_c} = h_c \frac{D_h}{k_L} = 0.087\ \mathrm{Re_m^{0.6}}\ \mathrm{Pr_L^{1/6}} \left(\frac{\rho_G}{\rho_L}\right)^{0.2} \left(\frac{k_W}{k_L}\right)^{0.09}, \quad [31]$$

with

$$\mathrm{Re_m} \triangleq \frac{\rho_L w D_h}{\mu_L}.$$

(c) *Johnson & Abou-Sabe correlation (1952).* When the phase change is only due to a longitudinal pressure gradient, these authors suggest the use of the following correlation:

$$h_{TP} = Z_G h_L \frac{\Psi^{0.1}}{(1-\alpha)^{0.9}}, \quad [32]$$

where

$$\Psi = \Phi_L^{3.33}(1-\alpha)^4,$$

$$Z_G = \left[1 + 0.006\left(\frac{\rho_m w D_h}{\mu_G}\right)^{0.5}\right]^{-1}$$

and h_L is calculated by the Dittus–Boelter correlation.

3.4. Critical Flow Condition and Compatibility Condition

3.4.1. Critical flow condition

The critical flow condition (Bouré *et al.* 1976) is the vanishing condition of the determinant of the set of equations [24]. It can be easily seen that this determinant is equal to its minor involving the three first lines and the three first columns. One obtains then

$$\left(\frac{w_c}{v_m}\right)^2 = -\left(\frac{\partial p}{\partial v_m}\right)_{s_m, y}. \quad [33]$$

The critical velocity w_c derived from the present model is thus identical to the classical expression of the speed of sound:

$$w_c = \sqrt{\left(\frac{\partial p}{\partial \rho_m}\right)_{s_m, y}}. \quad [34]$$

Here, the isentropic condition implies not only the absence of wall friction and wall heat flux, but also the absence of mass transfer inside the mixture, i.e. a constant value for y.

3.4.2. Compatibility condition

The compatibility condition is derived from the vanishing condition of a secondary determinant of the matrix of [24] at the critical section. This condition is necessary to guarantee a physical solution at the critical section. From [24], the compatibility equation is given by

$$\frac{v_m}{A}\left(\frac{w_c}{v_m}\right)^2 \frac{dA}{dz} - \frac{P_W}{A}\tau_W - \frac{\Delta_{ES}}{\dot{M}_c}\left(\frac{w_c}{v_m}\right)^2 \frac{\partial v_m}{\partial s_m} - f(p, y, T_{LM})\left(\frac{w_c}{v_m}\right)^2 \left(\frac{\partial v_m}{\partial y} + \frac{\Delta_{IS}}{\dot{M}_c}\frac{\partial v_m}{\partial s_m}\right) = 0. \quad [35]$$

Taking [20′] and [23] into account, the compatibility equation can be rewritten as

$$\frac{v_m}{A}\left(\frac{w_c}{v_m}\right)^2 \frac{dA}{dz} - \frac{P_W}{A}\tau_W - \left(\frac{w_c}{v_m}\right)^2 \left(\frac{\partial v_m}{\partial s_m}\frac{ds_m}{dz} + \frac{\partial v_m}{\partial y}\frac{dy}{dz}\right) = 0. \quad [36]$$

Further, as the expression of the gradient of the specific volume is

$$\frac{dv_m}{dz} = \frac{\partial v_m}{\partial p}\frac{dp}{dz} + \frac{\partial v_m}{\partial y}\frac{dy}{dz} + \frac{\partial v_m}{\partial s_m}\frac{ds_m}{dz}, \quad [37]$$

taking into account [33], [36] becomes

$$\frac{v_m}{A}\left(\frac{w_c}{v_m}\right)^2\frac{dA}{dz}-\frac{P_W}{A}\tau_W-\left(\frac{w_c}{v_m}\right)^2\left[\frac{dv_m}{dz}+\left(\frac{v_m}{w_c}\right)^2\frac{dp}{dz}\right]=0. \quad [38]$$

This equation is formally identical to the compatibility condition for a single-phase compressible flow. In particular, if this flow is frictionless and the cross section uniform, then [38] is reduced to

$$\frac{dp}{dv_m}=\left(\frac{\partial p}{\partial v_m}\right)_{s_m,y}. \quad [39]$$

However, just as in single-phase flow, this condition cannot be fulfilled at any section in the pipe under these circumstances: thus, the critical section is located at the pipe outlet. This conclusion holds in the case where $dA/dz < 0$.

4. CALCULATION PROCEDURE AND RESULTS

4.1. Calculation Procedure

A computer program has been developed to calculate the flow through the crack (critical or not) according to the model presented in section 3.

An iterative procedure is used in this computer program to converge towards the boundary conditions, i.e. at one end the inlet pressure and temperature of the subcooled water, and at the other end either the pressure of the secondary side when the critical regime is not achieved or [33] when the flow is critical.

This procedure works as follows:

1. Using [2] and [3], the first step consists of determining the flow rate, by assuming that the flow remains liquid throughout the depth of the crack (L_C), and by considering the outlet pressure, given by

$$p_0 = 0.97 p_S(T_{LM}).$$

2. The set of o.d.e.s. for three-phase flow is then integrated step by step using a Runge–Kutta adaptative method for the fourth order with the following initial conditions:

   —velocity w corresponding to the estimated flow rate
   —$X = 0$
   —$y = 0$
   —$p = p_0 = 0.97 p_S(T_{LM})$
   —$s_m = f(p_0, T_{LM})$.

   The integration is performed by means of pressure steps until either the critical flow conditions (the determinant of the matrix of the set of o.d.e.s. vanishes) or the outlet pressure is reached. This second step allows one to determine the distance L_{TP} of the three-phase flow zone for the given initial flow rate.
3. A new flow rate can now be calculated with the length of the single-phase (liquid) zone equal to $L_C - L_{TP}$ according to the procedure described in point 1 above.

This iteration is repeated until each of the following parameters converges within a given relative accuracy:

—flow rate
—lengths of single phase and/or three-phase flow zone
—quality X at the exit
—mass fraction y at the exit.

In order to evaluate the r.h.s. of the set of o.d.e.s., different correlations for the wall shear stress, [27]–[29], and for the wall heat transfer, [30]–[32], can be used.

The choice between these correlations is an option in the computer program.

A sensitivity study (see section 4.2.2) shows that the calculated mass flow rates are practically independent of the correlations used for the pressure drop and for the heat transfer in the three-phase flow. The assumption of an adiabatic flow leads to approximately the same results.

4.2. Comparison Between Experimental Data and the Present Model

Two types of tests with slits have been selected: (i) the John *et al.* (1988) tests; and (ii) the Amos (1983) tests.

4.2.1. John et al. (1988) tests

These tests have been chosen because their results are very coherent and seem to have been made in good conditions, even if the size of the slits are larger than the cracks we want to study.

The slits are rectangular and their dimensions are well known. The depth of the slits is 46 mm and the length 80 mm. The width ranges from 0.25 to 0.44 mm. Several roughnesses have been tested and range from 5.3 to 287 μm.

For each slit, some single-fluid flow experiments have been performed in cold water to determine the global friction factor. The results have been used without any adjustment to the computer program.

For each slit, two-phase flow tests have been done for different upstream pressures (40, 60, 80 and 100 bar), and, for each pressure, several upstream subcooled temperatures (2–60°C) have been tested. The exit pressure ranged from 4 to 9 bar.

More than 70 tests have been compared with the present model (figure 4). This model shows a reasonable agreement with the data (better than $\pm 12\%$). We note also that the present

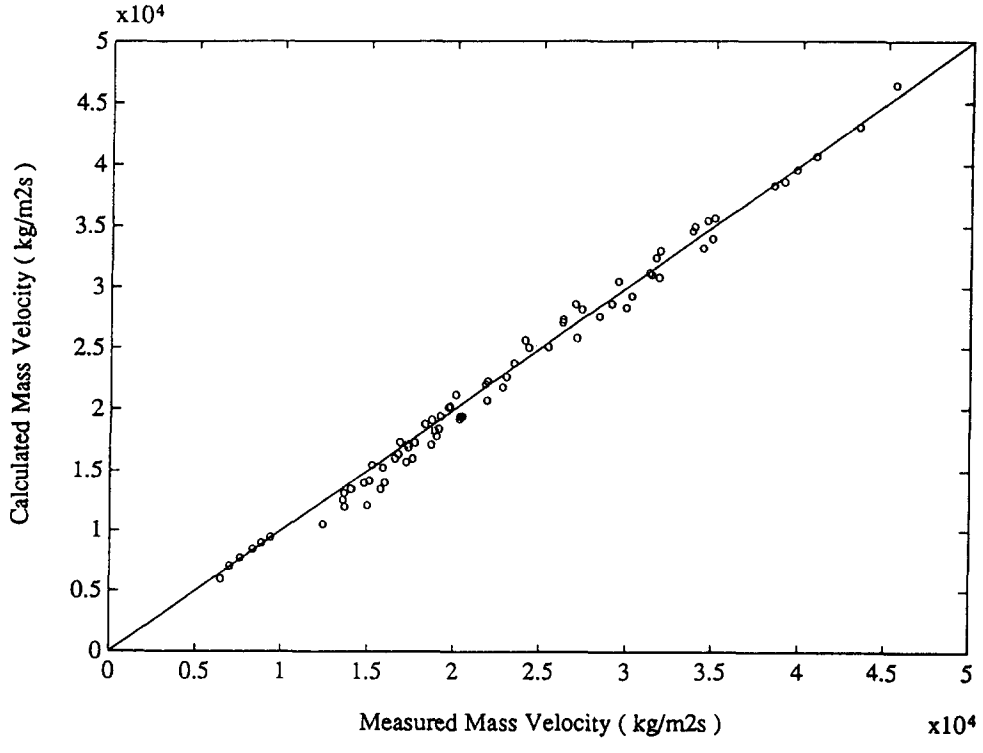

Figure 4. Comparison between the test results from John *et al.* (1988) and the present model.

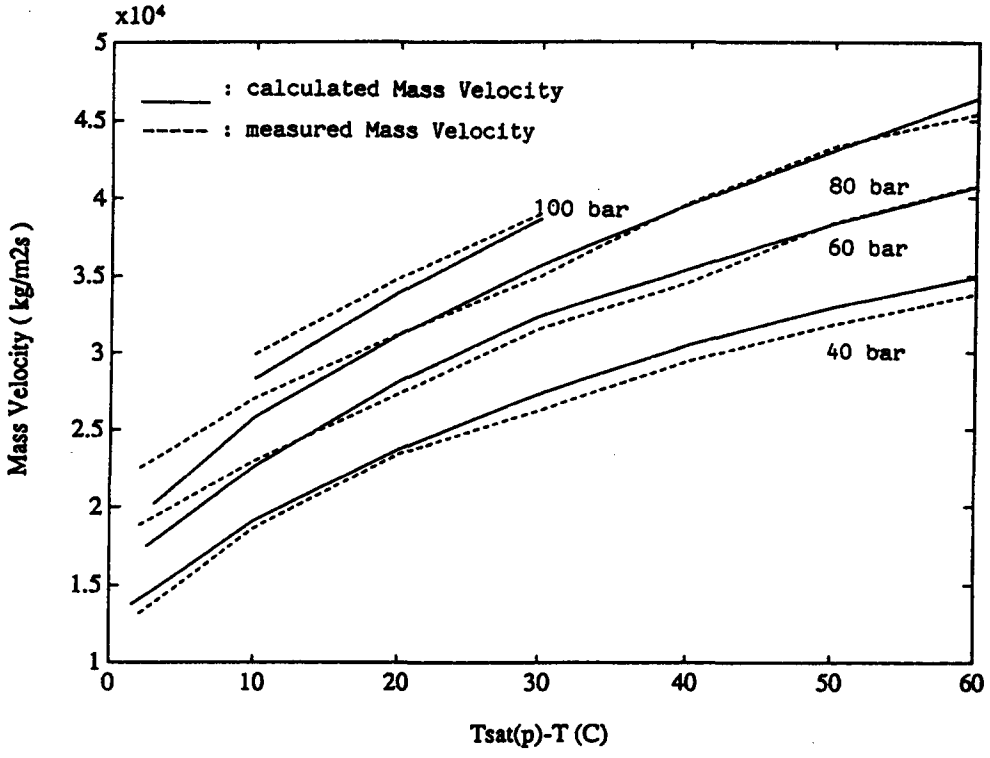

Figure 5. Critical mass velocity vs $T_{sat}(p) - T$ at the entrance of the channel for different inlet pressures: a comparison between the test results from John *et al.* (1988) and the present model.

model can fairly well reproduce the flow rate decrease with the subcooled temperature decrease (figure 5).

4.2.2. Amos (1983) tests

The tests have been carried out with real cracks whose dimensions are bigger than those we are interested in. The cracks had a depth of 63.5 mm, a length of about 20 mm and a width ranging from 0.127 to 0.381 mm. The thermohydraulic parameters are the upstream pressure ranging from 41 to 162 bar and the upstream subcooled temperature ranging from 0 to 65°C.

Table 2. Comparison between data from Amos (1983) and calculations using the present model

Run No.	p_e (MPa)	$\Delta T_{sat,c}$ (°C)	Wall roughness (m × 10^{-6})	ξ (—)	G_c experimental ((kg/m² s) × 10^4)	G_c calculated ((kg/m² s) × 10^4)	ΔG_c (%)
57	4.216	27.9	0.3	0.305	3.233	3.247	+0.4
58	4.176	14.4	0.3	0.305	2.513	2.523	+0.4
59	4.270	59.2	0.3	0.305	4.105	4.279	+4.2
27	7.073	29.5	0.3	0.177	4.256	4.146	−2.6
28	7.075	15.5	0.3	0.177	3.309	3.268	−1.2
30	7.096	62.8	0.3	0.177	5.737	5.517	−3.8
41	9.590	60.8	0.8	0.348	5.471	5.525	+1.0
42	11.583	56.0	0.8	0.348	5.518	5.744	+4.1
43	9.583	29.7	0.8	0.348	4.140	4.228	+2.1
44	9.628	14.3	0.8	0.348	3.228	3.266	+1.2
45	11.607	29.1	0.8	0.348	4.368	4.483	+2.6
74	15.413	54.7	0.3	0.316	6.995	6.787	−2.9
76	11.674	11.8	0.3	0.316	3.696	3.506	−5.1
78	15.433	25.6	0.3	0.316	4.805	5.026	+4.6

Nominal opening slit = 0.381 × 10^{-3} m. $\Delta G_c = \dfrac{G_{c\,calc} - G_{c\,exp}}{G_{c\,exp}} \times 100.$

Table 3. Comparison between data from Amos (1983) and calculations using the present model

Run No.	P_c (MPa)		P_{exp} (MPa)	ΔP_c (%)	
	Amos (1983)	Present model		Amos (1983)	Present model
57	2.423	1.963	2.047	+18.4	−4.0
58	3.148	2.421	2.387	+31.9	+1.4
59	1.286	1.081	1.313	−2.0	−17.6
27	4.197	3.341	2.970	+41.3	+12.5
28	5.342	4.057	3.400	+57.1	+19.0
30	2.265	1.904	1.878	+20.6	+1.4
41	3.377	2.805	3.552	−4.9	−21.0
42	4.310	3.780	4.478	−3.8	−15.6
43	5.730	4.505	4.820	+18.9	−6.5
44	6.756	5.406	5.264	+28.3	+2.7
45	7.196	5.543	5.997	+20.0	−7.6
74	6.423	5.405	6.135	+4.7	−11.9
76	7.634	6.769	5.905	+29.3	+14.6
78	10.350	7.858	7.613	+36.0	+3.2

Nominal opening slit $= 0.381 \times 10^{-3}$ m. $\Delta P_c = \dfrac{P_{c\,calc} - P_{c\,exp}}{P_{c\,exp}} \times 100.$

Tables 2 and 3 and figures 6–9 present the results of comparisons between the present model and 14 sets of data (width: 0.381 mm). As each set of data corresponds to an operation of dismounting and mounting the test section, the wall roughness and the inlet head loss coefficient had to be adjusted by means of cold water preliminary test results. The data used for the present comparison consist of averages calculated over several measurements made for each test run. The average relative deviation between the measured mass velocities $G_{c\,exp}$ and the calculated mass velocities $G_{c\,calc}$ obtained with the present model is similar (2.6%) to the deviation obtained by Amos & Schrock (1984) (2.4%), whereas, for the critical pressure, the deviation obtained with the present model is 9.9% instead of 22.6% with Amos & Schrock model. It is interesting to note in figures 6 and 7 and the pressure profiles are also correctly predicted. The improvement of such predictions with respect to the model proposed by Amos & Schrock (1984) is illustrated in figure 8.

A sensitivity analysis of the model has been checked for a typical test run (figure 9). We note that the wall heat transfer correlation has almost no effect on the predictions, whereas small effects are found when varying either the wall shear-stress correlation, the value of parameter k_1 used in [1], the wall roughness or the inlet head loss coefficient. On the contrary, the parameter k_2 which appears in the semi-empirical law governing the evolution of the non-equilibrium, strongly affects the results when it is varied by 2 orders of magnitude.

5. CONCLUSIONS

A new model for two-phase choked flow through cracks is proposed. It takes into account the thermal non-equilibrium which appears when initially subcooled water is released in a piston-like steady-state flow.

The crack is considered as a straight channel which can be uniform, convergent or divergent. Wall roughness is determined *a priori* by single-phase flow data because the *a priori* knowledge of the hydraulic characteristics of the cracks remains an unsolved issue. Wall heat flux and wall friction are calculated by classical single- and two-phase flow correlations.

The fluid is modelled as a three-phase mixture consisting of metastable liquid, saturated liquid and saturated vapour. The slip between the phases is neglected. The set of balance equations is written and complemented by a closure law for the irreversible mass transfer between the two liquid phases. This law appears to be an extension of the relaxation equation (Bilicki & Kestin 1990).

The critical flow conditions associated with the compatibility condition are found to be formally similar to single compressible flow results.

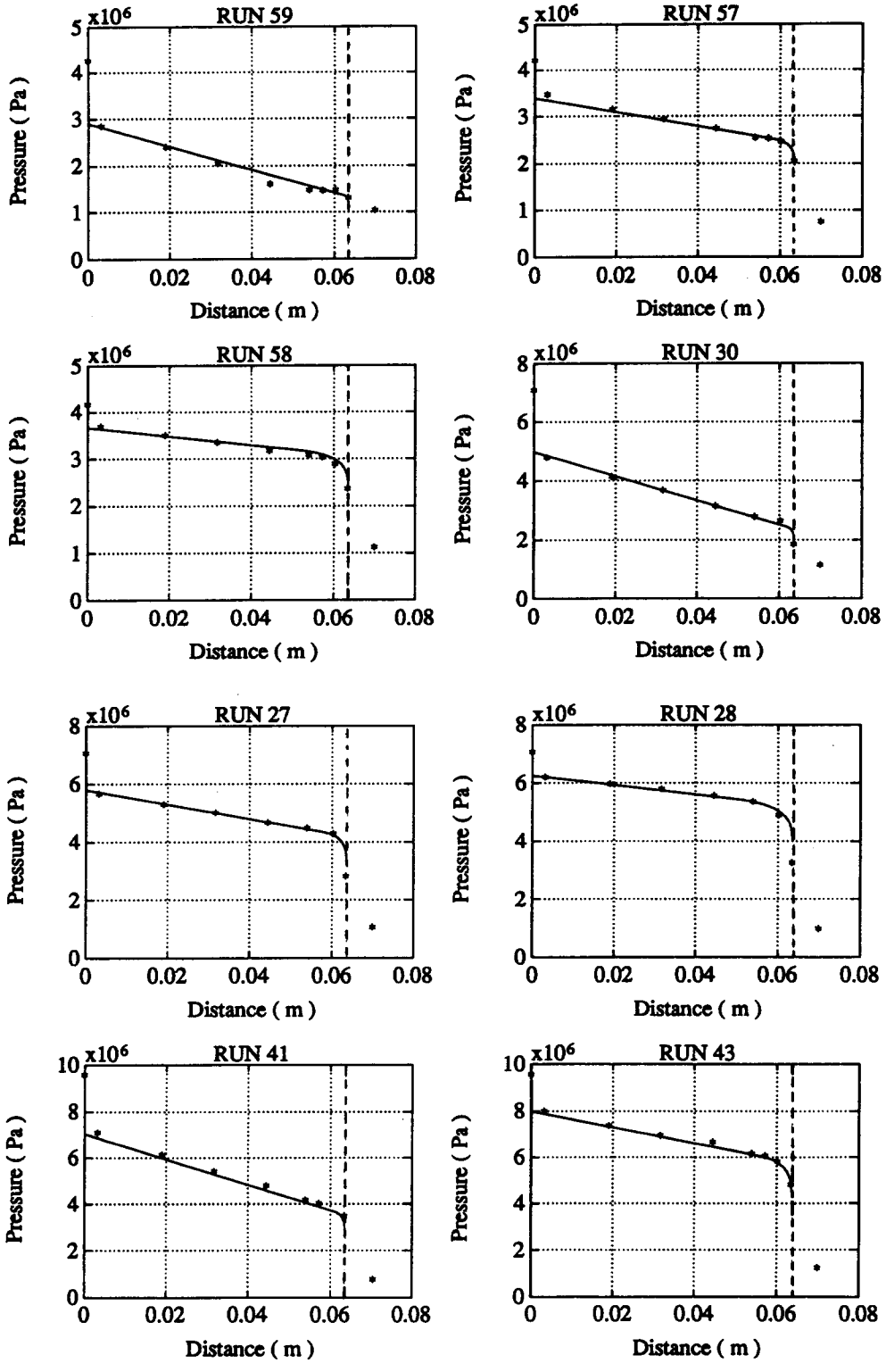

Figure 6. Pressure profiles: *, data from Amos (1983) tests; —, present model.

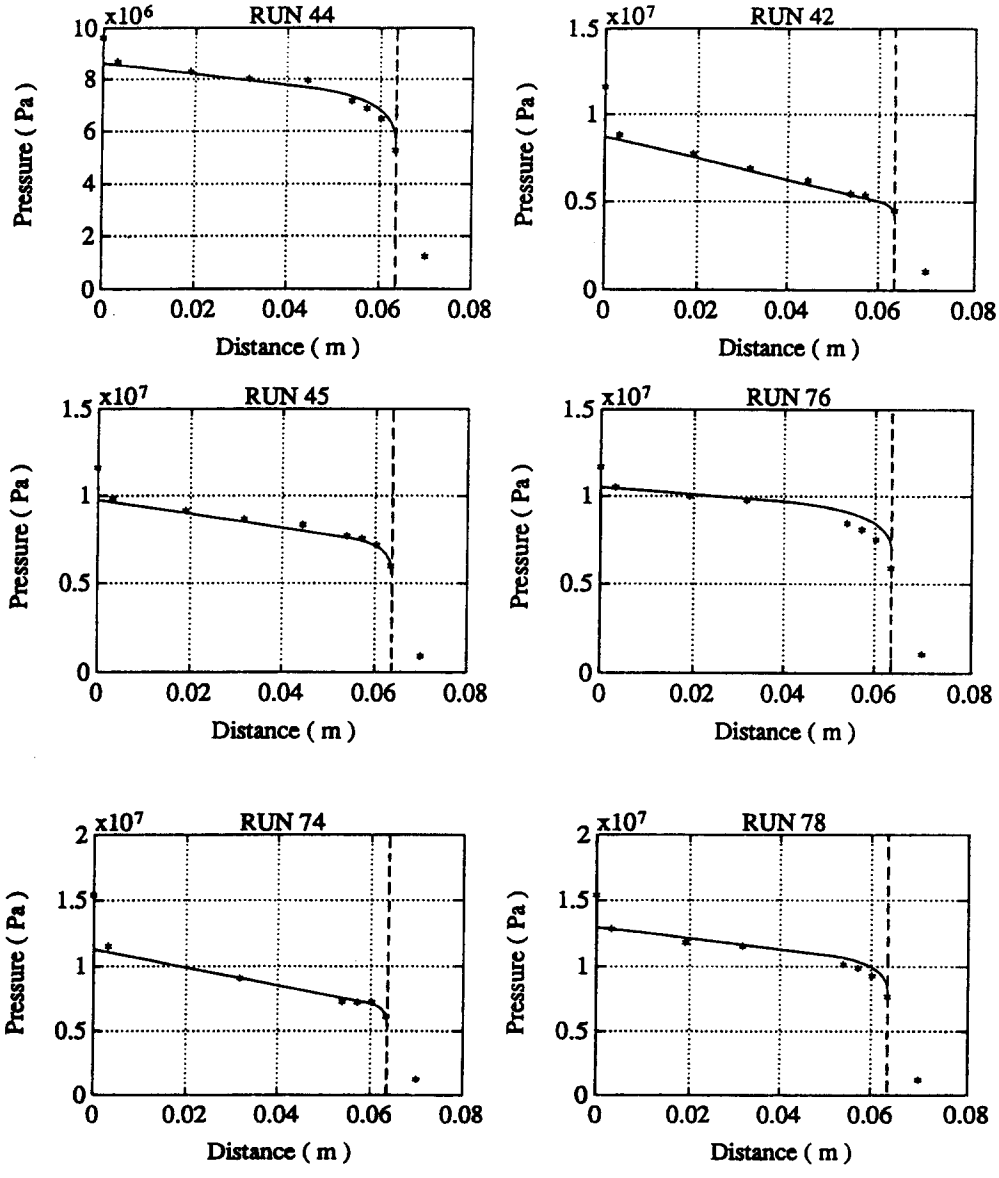

Figure 7. Pressure profiles: *, data from Amos (1983) tests; —, present model.

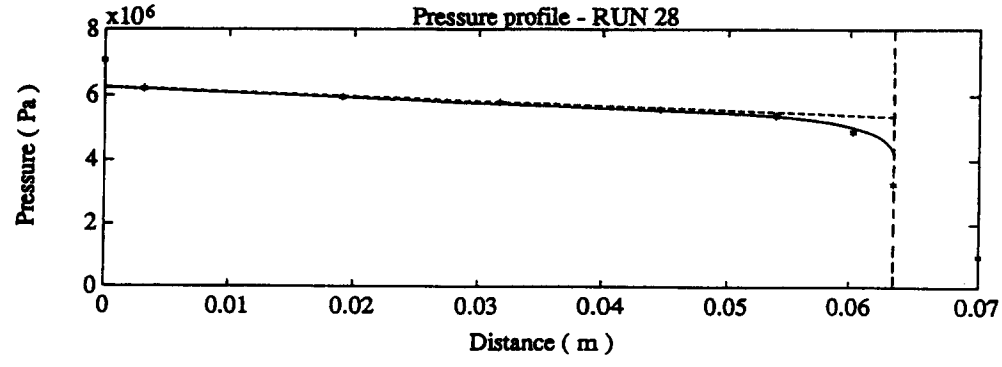

Figure 8. Pressure profiles: *, data from Amos (1983) with $G_c = 3.309 \times 10^4$ kg/m^2 s; —, present model with $G_c = 3.268 \times 10^4$ kg/m^2 s; ---, Amos & Schrock (1984) with $G_c = 3.369 \times 10^4$ kg/m^2 s.

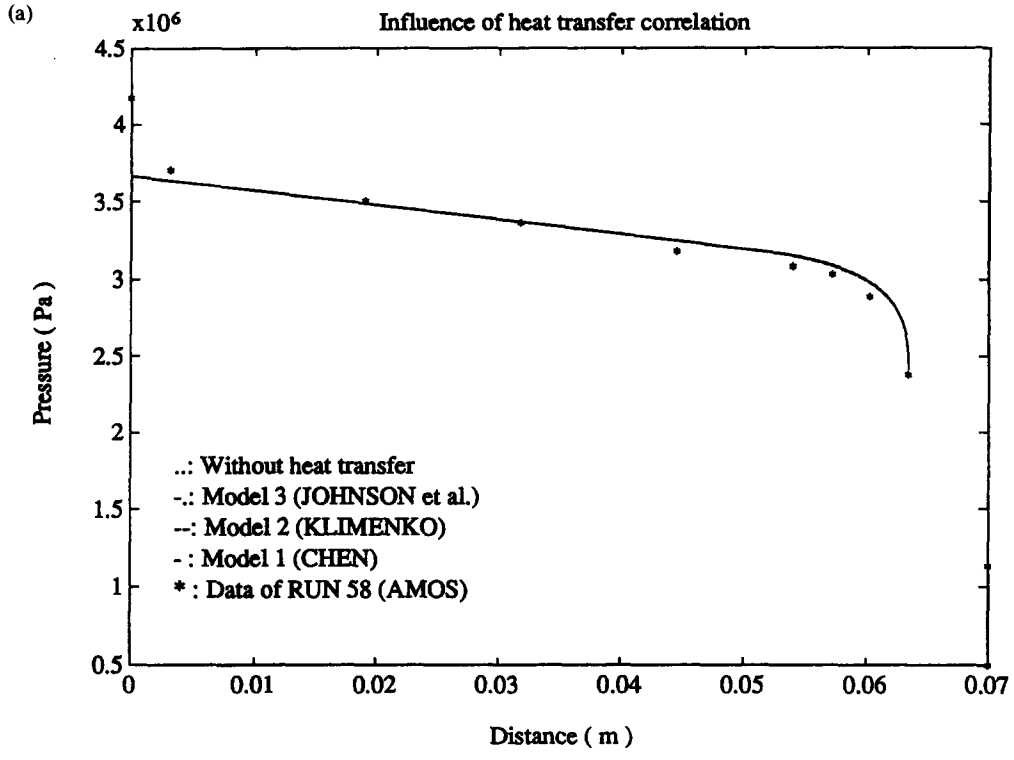

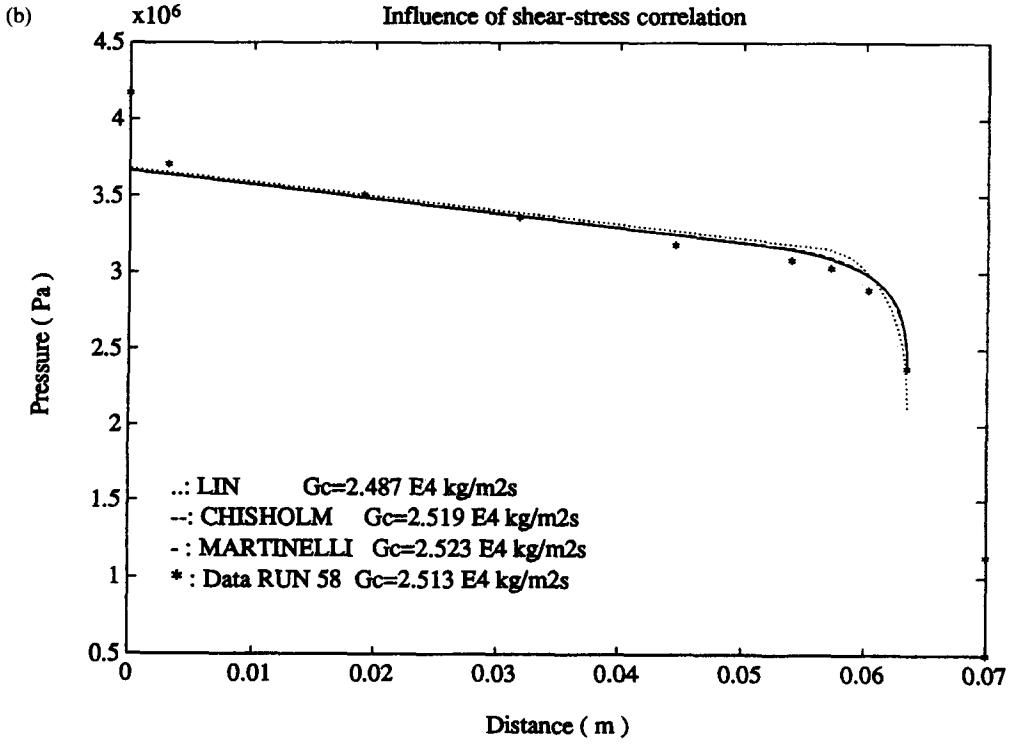

Figure 9—*caption on p. 561.*

(c)

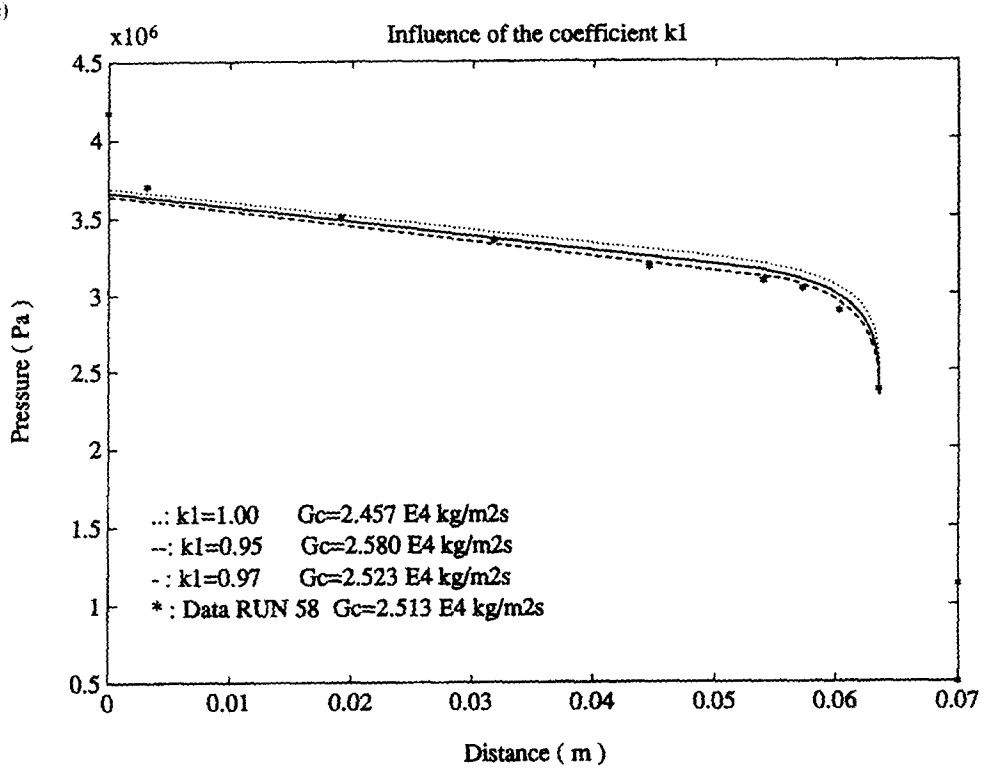

(d)

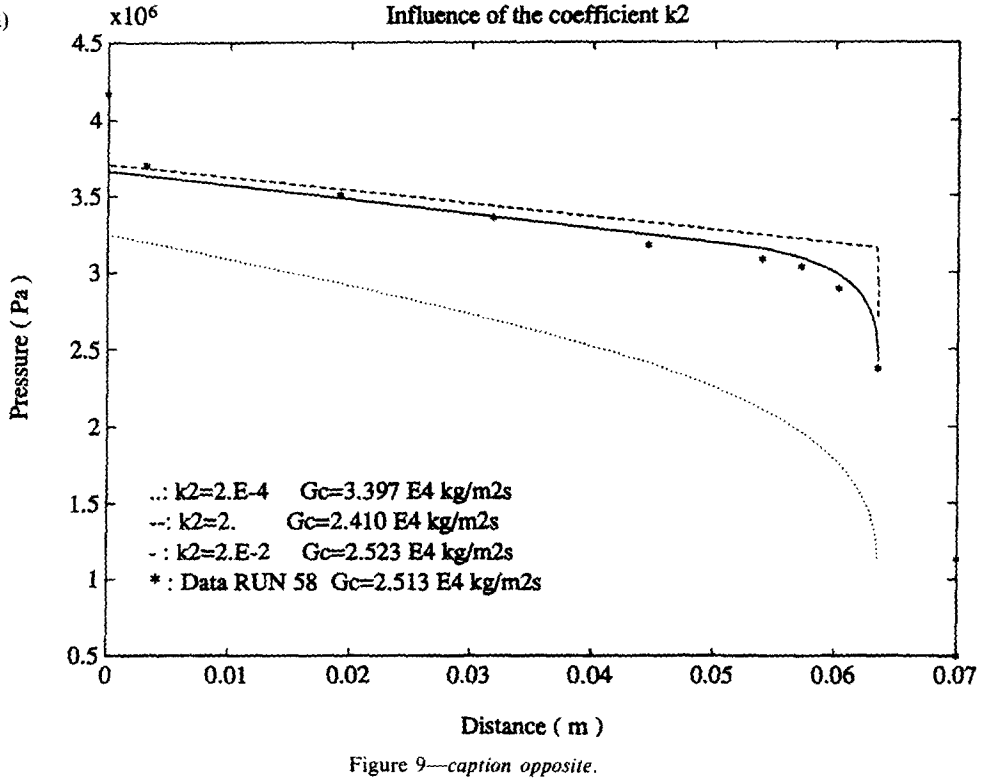

Figure 9—*caption opposite.*

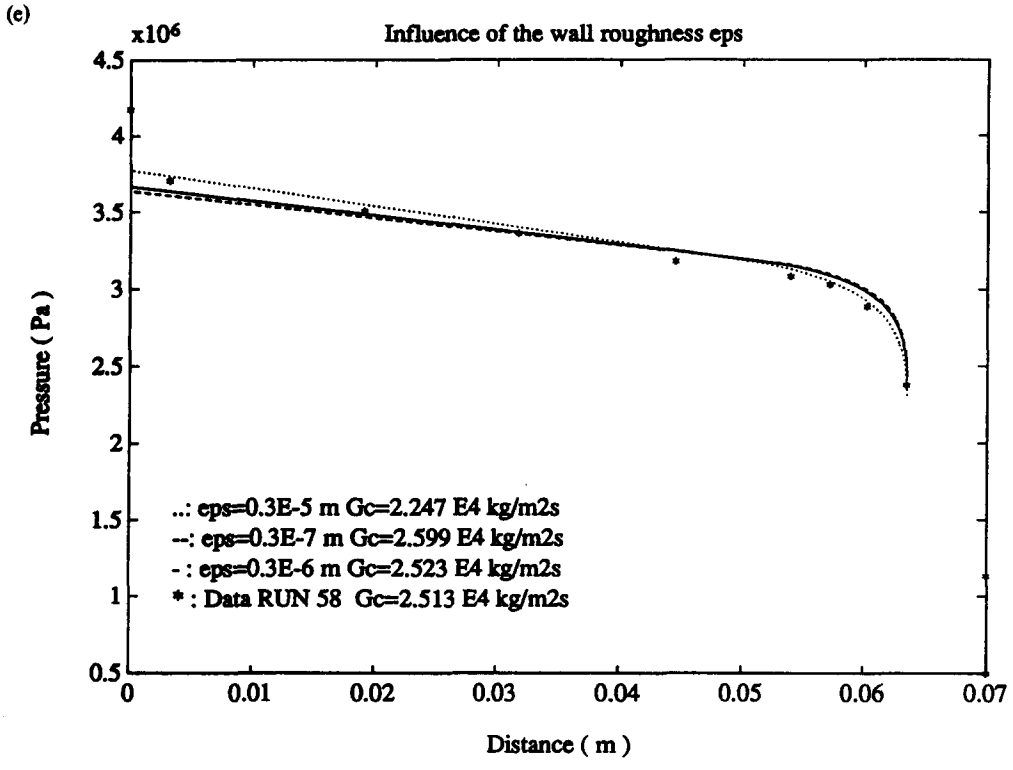

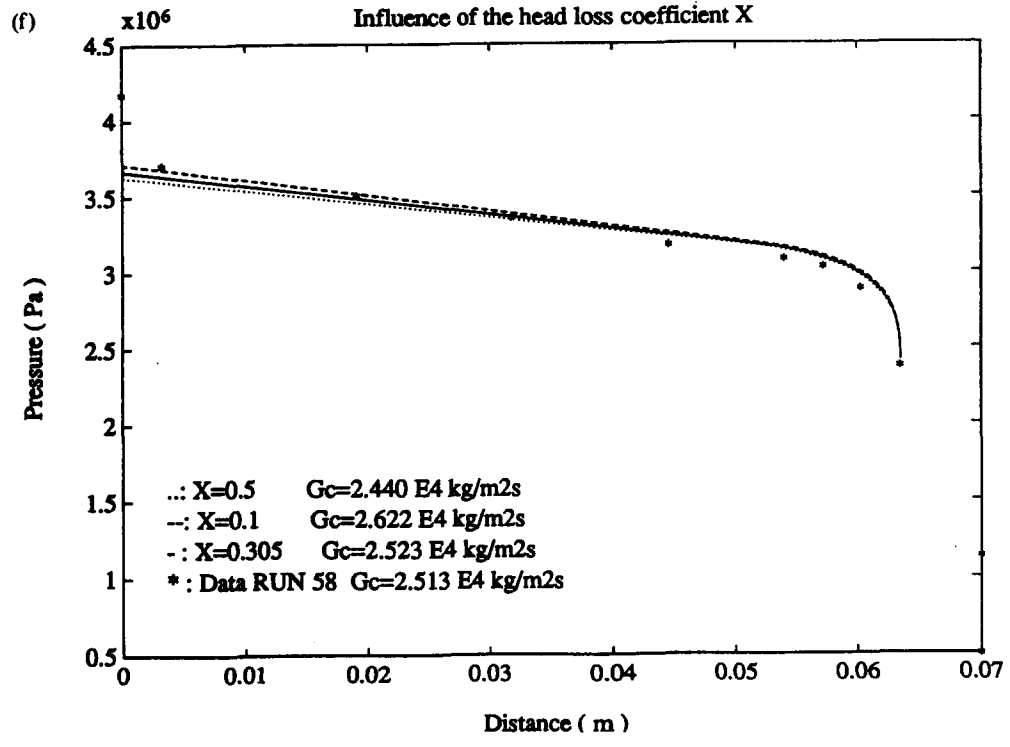

Figure 9. Sensitivity analysis; influence of (a) heat transfer correlation, (b) shear-stress correlation, (c) coefficient k_1, (d) coefficient k_2, (e) wall roughness and (f) head loss coefficient at the inlet.

The model is implemented in a computer program designed for the simulation of steam-generator small leaks. The results have been compared with some data published by John *et al.* (1988) and Amos (1983). Good agreement has been found between the present results and the experimental data. The validation will proceed further for smaller cracks using a new test facility currently under construction at EDF.

Acknowledgement—The authors thank Ir. G. De Pelsemaeker for his fruitful cooperation in the development of the computer program.

REFERENCES

ALAMGIR, M. & LIENHARD, J. H. 1981 Correlation of pressure undershoot during hot-water depressurization. *J. Heat Transfer* **103,** 52–55.

AMOS, C. N. 1983 Critical discharge of initially subcooled water through slits. Ph.D. Thesis, Univ. of California, Berkeley.

AMOS, C. N. & SCHROCK, V. E. 1984 Two-phase critical flow in slits. *Nucl. Sci. Engng* **88,** 261–274.

BILICKI, Z. & KESTIN, J. 1990 Physical aspects of the relaxation model in two-phase flow. *Proc. R. Soc. Lond.* **A428,** 379–397.

BILICKI, Z., KESTIN, J. & PRATT, M. M. 1990 A reinterpretation of the results of the Moby Dick experiments in terms of the non-equilibrium model. *Trans. ASME* **112,** 212–217.

BOURE, J. A., FRITTE, A. A., GIOT, M. M. & REOCREUX, M. L. 1976 Highlights of two-phase critical flow. *Int. J. Multiphase Flow* **3,** 1–22.

CHEN, J. C. 1966 A correlation for boiling heat transfer to saturated fluids in convective flow. *Ind. Chem. Engng Process Des. Dev.* **5,** 322–329.

CHURCHILL, S. W. 1977 Friction factor equation spans all fluid flow regimes. *Chem. Engng* **84,** 91.

FAUSKE, H. K. 1962 Contribution to the theory of two-phase, one component critical flow. Report ANL-6633.

GIOT, M. & MEUNIER, D. 1968 Méthodes de détermination du débit critique en écoulements monophasiques et diphasiques à un constituant. *Energie Primaire* **4,** 47–67.

HARDY, Ph. & MALI, P. 1983 Validation & development of a model describing subcooled critical flows through long tubes. *Energie Primaire* **18,** 5–23.

JOHN, H., REIMANN, J., WESTPHAL, L. & FRIEDEL, L. 1988 Critical two-phase flow through rough slits. *Int. J. Multiphase Flow* **2,** 155–174.

JOHNSON, H. A. & ABOU-SABE, A. H. 1952 Heat transfer and pressure drop for turbulent flow of air–water mixtures in a horizontal pipe. *Trans. ASME* 977–987.

KLIMENKO, V. V. 1988 A generalized correlation for two-phase forced flow heat transfer. *Int. J. Heat Mass Transfer* **31,** 541–552.

LACKMÉ, C. 1979 Incompleteness of the flashing of supersaturated liquid and sonic ejection of the produced phases. *Int. J. Multiphase Flow* **5,** 131–141.

LIN, S., KWOK, C., LI, R. Y., CHEN, Z. H. & CHEN, Z. Y. 1989 Local frictional pressure drop during vaporisation of R.12 through capillary tubes. Internal Report, Shanghai Inst. of Mechanical Engineering.

MOODY, F. J. 1965 Maximum flow-rate of a single component two-phase mixture. *J. Heat Transfer* **87,** 134–142.

NABAYASHI, T., FUJII, M., MATSUMOTO, K., NAKAMURA, S., TANAKA, Y. & HORIMUZU, Y. 1991 Experimental study on leak flow model through fatigue crack in pipe. *Nucl. Engng Des.* **128,** 17–27.

PANA, P. 1976 Berechnung der Stationären Massenstromdichte von Wasserdampfgewischen und der Auftretenden Rüchstrasskräfte. Report IRS-W-24.

YAN, F., GIOT, M. & BOLLE, L. 1990 Modelling of flashing during adiabatic release through pipes. In *Proc. EUROTHERM Semin., No. 14,* Louvain-la-Neuve, Belgium, Vol. 2, pp. 8-1/8-14.

YAN, F., BOLLE, L., FRANCO, J. & GIOT, M. 1991a Analysis of choked liquid–vapor flows. In *Proc. Multiphase Flows '91,* Tsukuba, Japan, pp. 309–312.

YAN, F., GIOT, M. & BOLLE, L. 1991b Mechanism of bubble generation in adiabatic vessels and pipes: experimental and theoretical study. In *Phase Change Heat Transfer; ASME HTD-159,* pp. 149–156. ASME, New York.